Popular Strains: Characteristic Features and Their Use for Research

Table 2 shows the mouse strains which are requested by many researchers. A recent trend is that requests for Cre mice are increasing substantially due to the performance of its conditional knockout.

Among Cre mice, P0-Cre is one of the most frequently requested strains. Although this strain of mouse has been described in a published manuscript [10], we would like to briefly introduce the characteristics of this mouse. Neural crest cells are embryonic, multipotent stem cells that give rise to various cell/tissue types and thus serve as a good model system for the study of cell specification and mechanisms of cell differentiation. For analysis of neural crest cell lineage, transgenic mice harboring a Cre gene driven by a promoter of protein 0 (P0) were generated. To detect and visualize the Cre-mediated DNA recombination in neural crest cells and derivatives, we utilized another transgenic (Tg) line with the CAG-CAT-Z indicator construct [10]. This Tg line carries a *lacZ* reporter gene downstream of a chicken β-actin promoter and a "stuffer" fragment flanked by two *loxP* sequences. The *lacZ* is expressed only when the stuffer is removed by the action of Cre recombinase. Using these transgenic mice, we demonstrated that a subset of migrating neural crest cells and a wide variety of cells in the neural crest cell lineage could be marked by *lacZ* expression. Thus, the use of this system may facilitate many interesting experiments, including lineage analysis, purification, and manipulation of the mammalian neural crest cells. Also, this cell-type-specific transgenesis system should facilitate functional analysis of genes of interest in the neural crest cell lineage. Up to now, this strain of mouse has been used in many studies and is now one of the most useful Cre-driver mice.

Deposition and Request for Mouse Strains and EGTC

An outline of the deposition and request procedures for mouse strains is illustrated in Fig. 1. Information on the application procedure is available on the web page (Fig. 2) (http://card.medic.kumamoto-u.ac.jp/card/english/index.html). As we are one of the founding members of FIMRe (http://www.fimre.org/), we also offer our mouse data to the integrated database IMSR (International Mouse Strain Resources) (http://www.informatics.jax.org/imsr/index.jsp). Thus, researchers also can find mouse strains using these databases.

Table 2. Frequently requested mouse strains

ID: 148	C57BL/6J-Tg(PO-Cre)94Imeg
ID: 250	Tg(K5-Cre)
ID: 709	B6;C3H-Tg(K19-Wnt1/K19-Ptgs2/K19-Ptges)
ID: 428	C57BL/6N-Tg(CAG-AURKA(WT)Card
ID: 196	B6;129-Synd4^{tm1}
ID: 189	Tg(E/nestin:EGFP-50)
ID: 175	Tg(E/nestin:EGFP-25)
ID: 91	Tg(CAG-Cre)
ID: 89	Tg(lck-Cre)
ID: 509	B6;D2-Tg(CAG-CAT-EGFP)39Miya
ID: 355	C57BL/6-CD9^{tm1};Tg(ZP3-EGFPCD9)
ID: 312	B6;CB-Dtr$^{tm2(lox)}$
ID: 290	C57BL/6 -Tg(Act-EGFP)C14-Y01-FM131Osb
ID: 88	C57BL/6-Rag1$^{tm1(GFP)Imku}$

Major Achievement: Publication

More than 150 studies using genetically engineered mice produced by CARD, have been published so far. Among these some representative manuscripts are listed in Table 3. This list clearly suggests that technical services in mouse embryo manipulation and reproductive engineering contribute greatly to the promotion of science.

Related Information

JMSR (http://www.shigen.nig.ac.jp/mouse/jmsr/top.jsp): The Japan Mouse/Rat Strain Resources Database (JMSR) is a searchable online database of mouse/rat strains and stocks available in Japan. The JMSR was developed in 2001 through discussions with the Mouse Genetic Resources Subcommittee (http://www.shigen.nig.ac.jp/shigen/grc/grc_mouse.jsp). The objective of this database is to provide a portal site which will help users to locate and obtain mouse/rat resources. This site is maintained by the Genetic Informatics Laboratory, National Institute of Genetics in close cooperation with data providers.

IGTC (http://www.genetrap.org/): The International

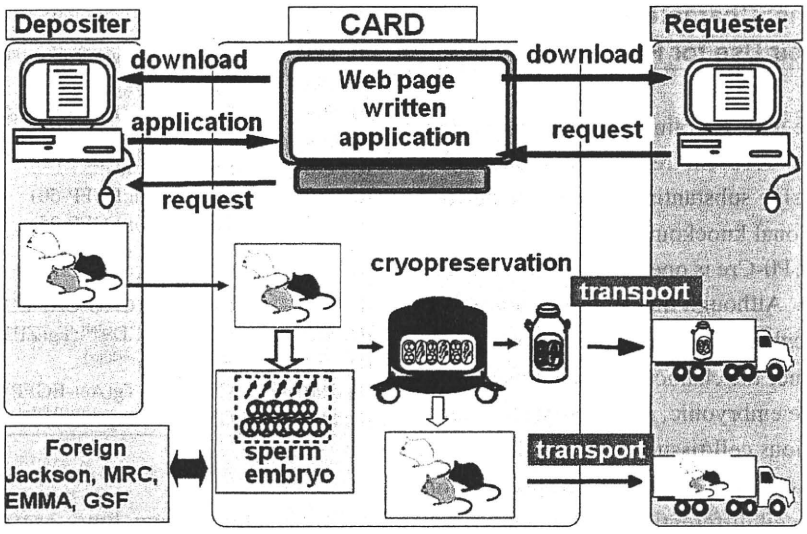

Fig. 1. Outline of deposition and request procedures for mouse strains. Information on the application procedure and necessary documents are available on the web page. Mouse embryos or sperm obtained from mice sent from depositors are cryopreserved and stored in liquid nitrogen tanks. Frozen embryos or live mice obtained by transfer of thawed embryos into foster mothers can be sent to requesters.

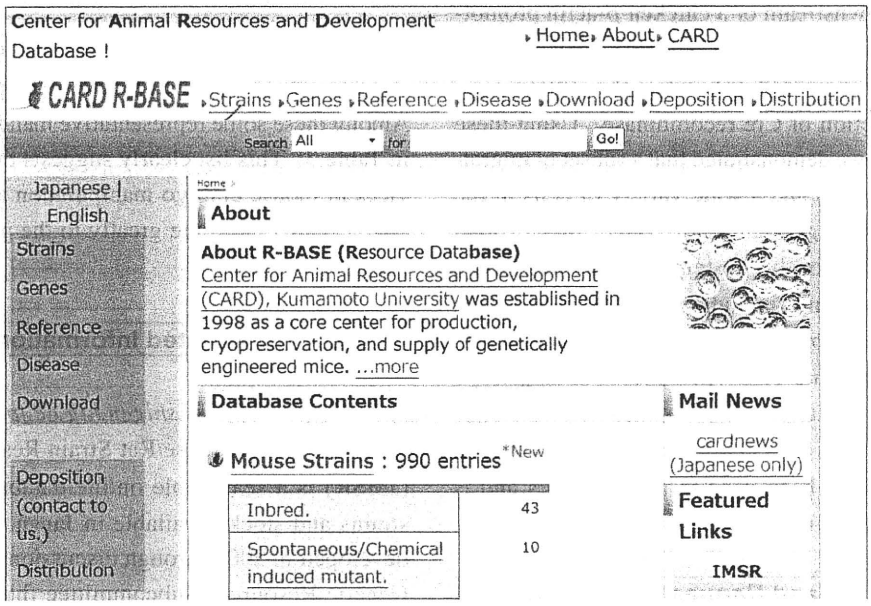

Fig. 2. Web page of CARD R-BASE. Only part of the web page is shown in this figure. Both Japanese and English versions are available.

Gene Trap Consortium (IGTC) consists of laboratories around the world working together to generate a public library of mutated murine ES cell lines. Such cell lines can be obtained on a non-collaborative basis by scientists interested in generating reporter-tagged, loss-of-function mutations in mice. In addition to loss of function, new-

Table 3. Selected publications

Ohnishi, N. *et al. Proc. Natl. Acad. Sci. U.S.A.* 105: 1003–1008, 2008.
Sato, T. *et al. Nature* 448: 366–369, 2007.
Imai, T. *et al. Science* 314: 657–661, 2006.
Serizawa, S. *et al. Cell* 127: 1057–1069, 2006.
Shim, J.H. *et al. Genes Dev.* 19: 2668–2681, 2005.
Terada, K. *et al. EMBO J.* 24: 611–622, 2005.
Tachibana, M. *et al. Genes Dev.* 19: 815–826, 2005.
Ohmuraya, M. *et al. Gastroenterology* 129: 696–705, 2005.
Itoh, H. *et al. Gastroenterology* 127: 1423–1435, 2004.
Yamazaki, S. *et al. J. Cell Biol.* 163: 469–475, 2003.
Ishida, D. *et al. Cancer Cell* 4: 55–65, 2003.
Serizawa, S. *et al. Science* 302: 2088–2094, 2003.
Wakabayashi, Y. *et al. Nat. Immunol.* 4: 533–539, 2003.
Yokosuka, T. *et al. J. Exp. Med.* 195: 991–1001, 2002.
Pepys, M.B. *et al. Nature* 417: 254–259, 2002.
Tachibana, M. *et al. Genes Dev.* 16: 1779–1791, 2002.
Yamauchi, T. *et al. Nat. Genet.* 30: 221–226, 2002.
Hasegawa, S. *et al. Proc. Natl. Acad. Sci. U.S.A.* 99: 297–302, 2002.
Yamaguchi, S. *et al. Nature* 409: 684, 2001.
Nishimura, H. *et al. J. Exp. Med.* 191: 157–169, 2000.
Hisahara, S. *et al. EMBO J.* 19: 341–348, 2000.
Nakai, A. *et al. EMBO J.* 19: 1545–1554, 2000.
McIlroy, D. *et al. Gene. Dev.* 14: 549–558, 2000.
Serizawa, S. *et al. Nat. Neurosci.* 3: 687–692, 2000.
Ishiguro, K. *et al. J. Clin. Invest.* 106: 873–878, 2000.
Shinkura, R. *et al. Nat. Genet.* 22: 74–77, 1999.
Terauchi, Y. *et al. Nat. Genet.* 21: 230–235, 1999.
Watanabe, N. *et al. J. Exp. Med.* 190: 461–469, 1999.
Ihara, Y. *et al. Proc. Natl. Acad. Sci. U.S.A.* 95: 2526–2530, 1998.
Fujii, H. *et al. EMBO J.* 17: 6551–6557, 1998
Watanabe, D. *et al. Cell* 95: 17–27, 1998.
Sawada, S. *et al. J. Exp. Med.* 187: 1439–1449, 1998.

er gene trap vectors offer a variety of post-insertional modification strategies to allow for the generation of other experimental alleles. The cooperative goal of the IGTC is to generate an international resource representing all or most genes in the mouse genome, and to provide the bioinformatics and logistical support to make the resource valuable and available to scientists.

IMSR (http://www.informatics.jax.org/imsr/index.jsp): The International Mouse Strain Resources (IMSR) is a searchable online database of mouse strains and stocks available worldwide, including inbred, mutant, and genetically engineered mice. The goal of the IMSR is to assist the international scientific community in locating and obtaining mouse resources for research. The data content found in the IMSR is as it was supplied by data provider sites.

EUCOMM (http://www.eucomm.org/): The European Conditional Mouse Mutagenesis Integrated Project (EUCOMM) is funded by the European Union Framework 6 programme. The goal of EUCOMM is to generate a collection of up to 13,000 mutated genes in mouse C57BL/6N embryonic stem (ES) cells using conditional gene trapping and gene targeting approaches. This library will enable mouse mutants to be established worldwide in a standardized and cost-effective manner, making mouse mutants available to a much wider biomedical research community than has been possible previously.

NorCOMM (http://norcomm.phenogenomics.ca/): NorCOMM (North American Conditional Mouse Mutagenesis project) is a large-scale research initiative focused on developing and distributing a library of mouse embryonic stem (ES) cell lines carrying single conditional knockout mutations across the mouse genome.

KOMP (http://www.nih.gov/science/models/mouse/knockout/): The Knockout Mouse Project is a trans-NIH initiative that aims to generate a comprehensive and public resource comprised of mouse embryonic stem (ES) cells containing a null mutation in every gene in the mouse genome.

References

1. Araki, K., Araki, M., and Yamamura, K. 2002. Site-directed integration of the cre gene mediated by Cre recombinase using a combination of mutant lox sites. *Nucleic Acids Res.* 30: e103.
2. Araki, K., Imaizumi, T., Sekimoto, T., Yoshinobu, K., Yoshimuta, J., Akizuki, M., Miura, K., Araki, M., and Yamamura, K. 1999. Exchangeable gene trap using the Cre/mutated lox system. *Cell. Mol. Biol. (Noisy-le-grand)* 45: 737–750.
3. Davisson, M. 2006. FIMRe: Federation of International Mouse Resources: global networking of resource centers. *Mamm. Genome* 17: 363–364.
4. Gordon, J.W., Scangos, G.A., Plotkin, D.J., Barbosa, J.A., and Ruddle, F.H. 1980. Genetic transformation of mouse embryos by microinjection of purified DNA. *Proc. Natl. Acad. Sci. U.S.A.* 77: 7380–7384.
5. Nakagata, N. 2000. Cryopreservation of mouse spermatozoa. *Mamm. Genome* 11: 572–576.
6. Nakao, K., Nakagata, N., and Katsuki, M. 1997. Simple and efficient vitrification procedure for cryopreservation of mouse embryos. *Exp. Anim.* 46: 231–234.
7. Nord, A.S., Chang, P.J., Conklin, B.R., Cox, A.V., Harper, C.A., Hicks, G.G., Huang, C.C., Johns, S.J., Kawamoto, M., Liu, S., Meng, E.C., Morris, J.H., Rossant, J., Ruiz, P., Skarnes, W.C., Soriano, P., Stanford, W.L., Stryke, D., von Melchner, H., Wurst, W., Yamamura, K., Young, S.G., Babbitt, P.C., and Ferrin, T.E. 2006. The International Gene Trap Consortium Website: a portal to all publicly available gene trap cell lines in mouse. *Nucleic Acids Res.* 34: D642–648.
8. Schwartzberg, P.L., Goff, S.P., and Robertson, E.J. 1989. Germ-line transmission of a c-abl mutation produced by targeted gene disruption in ES cells. *Science* 246: 799–803.
9. Taniwaki, T., Haruna, K., Nakamura, H., Sekimoto, T., Oike, Y., Imaizumi, T., Saito, F., Muta, M., Soejima, Y., Utoh, A., Nakagata, N., Araki, M., Yamamura, K., and Araki, K. 2005. Characterization of an exchangeable gene trap using pU-17 carrying a stop codon-beta geo cassette. *Dev. Growth Differ.* 47: 163–172.
10. Yamauchi, Y., Abe, K., Mantani, A., Hitoshi, Y., Suzuki, M., Osuzu, F., Kuratani, S., and Yamamura, K. 1999. A novel transgenic technique that allows specific marking of the neural crest cell lineage in mice. *Dev. Biol.* 212: 191–203.

Laboratory Investigation (2010) 90, 654–664

Relationship of strain-dependent susceptibility to experimentally induced acute pancreatitis with regulation of Prss1 and Spink3 expression

Jun Wang[1], Masaki Ohmuraya[1,2,3], Koichi Suyama[1,3], Masahiko Hirota[3], Nobuyuki Ozaki[1,3], Hideo Baba[3], Naomi Nakagata[4], Kimi Araki[1] and Ken-ichi Yamamura[1]

To analyze susceptibility to acute pancreatitis, five mouse strains including Japanese Fancy Mouse 1 (JF1), C57BL/6J, BALB/c, CBA/J, and C3H/HeJ were treated with either a cholecystokinin analog, cerulein, or a choline-deficient, ethionine-supplemented (CDE) diet. The severity of acute pancreatitis induced by cerulein was highest in C3H/HeJ and CBA/J, moderate in BALB/c, and mildest in C57BL/6J and JF1. Basal protein expression levels of the serine protease inhibitor, Kazal type 3 (Spink3) were higher in JF1 and C57BL/6J mice than those of the other three strains under normal feeding conditions. After treatment with cerulein, expression level of Spink3 increased remarkably in JF1 and mildly in C57BL/6J, BALB/c, CBA/J, and C3H/HeJ strains. Increased proteinase, serine, 1 (Prss1) protein expression accompanied by increased trypsin activity with cerulein treatment was observed in susceptible strains such as CBA/J and C3H/HeJ. Similar results were obtained with a CDE diet. In the 3 kb Spink3 promoter region, 92 or 8 nucleotide changes were found in JF1 or C3H *vs* C57BL/6J, respectively, whereas in the Prss1 promoter region 39 or 46 nucleotide changes were found in JF1 or C3H *vs* C57BL/6J, respectively. These results suggest that regulation of Prss1 and Spink3 expression is involved in the susceptibility to experimentally induced pancreatitis. The JF1 strain, which is derived from the Japanese wild mouse, will be useful to examine new mechanisms that may not be found in other laboratory mouse strains.
Laboratory Investigation (2010) **90,** 654–664; doi:10.1038/labinvest.2010.44; published online 15 February 2010

KEYWORDS: serine protease inhibitor, Kazal type 3 (Spink3); proteinase, serine, 1 (Prss1); single-nucleotide polymorphisms (SNPs)

Over 450 inbred strains of mice have been described,[1] providing a wealth of different genotypes and phenotypes for studying human diseases. Actually, the use of various breeding strategies in combination with positional cloning and positional candidate gene approach has led to the discovery of many genes that underlie human disease.[2] The Japanese wild mouse, belonging to *Mus musculus molossinus*, has several genetic characteristics clearly distinguishable from the European wild mouse, derived from *M.m. domesticus*. These subspecies were separated about one million years ago and about 1% of their genome sequences are different.[3–8] Therefore, strains MSM/Ms[9] and Japanese Fancy Mouse 1 (JF1),[10] which were established from *M.m. molossinus*, are powerful genetic resources to analyze disease processes.

Many inbred strains have been bred for specific phenotypes. C57BL/6J mice are susceptible to high-fat diet-induced type II diabetes.[11] JF1 mice are especially sensitive to high-fat diet-induced diabetes and obesity, whereas MSM/Ms mice are resistant.[12] To date, however, there is little information about the difference in severity of pancreatitis among inbred strains of mice.

Acute pancreatitis is an important disease that can be triggered by a variety of factors, including excessive alcohol consumption,[13–16] obstruction of the ampulla of Vater by gall stones,[17,18] and genetic factors.[19,20] Hereditary chronic pancreatitis is a rare form of early onset chronic pancreatitis, characterized by the onset of recurrent attacks of acute pancreatitis in childhood, and frequently progresses to chronic pancreatitis. One type of the hereditary pancreatitis is caused by a mutation in the proteinase, serine, 1 (PRSS1) gene, encoding cationic trypsinogen. PRSS1 mutation results in an amino-acid substitution in the autolytic domain of

[1]Division of Developmental Genetics, Institute of Molecular Embryology and Genetics, Kumamoto University, Kumamoto, Japan; [2]Priority Organization for Innovation and Excellence, Kumamoto University, Kumamoto, Japan; [3]Department of Gastroenterological Surgery, Kumamoto University, Kumamoto, Japan and [4]Center for Animal Resources and Development, Institute of Resource Development and Analysis, Kumamoto University, Kumamoto, Japan
Correspondence: Dr K-i Yamamura, MD, PhD, Institute of Molecular Embryology and Genetics, Kumamoto University, 2-2-1 Honjo, Kumamoto 860-0811, Japan.
E-mail: yamamura@gpo.kumamoto-u.ac.jp

Received 18 August 2009; revised 13 January 2010; accepted 13 January 2010

trypsin. Thus, the mutation blocks autolysis and results in continuous trypsin activity.[21,22] In addition, mutation of the trypsin-specific inhibitor, serine protease inhibitor, Kazal type 1 (SPINK1), has been found to be associated with chronic pancreatitis as well.[23] We earlier showed that Spink3 (mouse homolog of human SPINK1) has dual functions for trypsin inhibition: one as a trypsin inhibitor by direct binding to trypsin[24] and another as a suppressor of autophagy, which is involved in trypsinogen activation.[25,26] In summary, mutations in PRSS1[27] and SPINK1[19] genes are acknowledged as genetic risk factors for pancreatitis in human patients.

To address whether genetic background can affect the development of acute pancreatitis in relation to expression of Prss1 and Spink3, the susceptibility of acute pancreatitis was compared among five inbred mouse strains including JF1 in two models of experimental acute pancreatitis, cerulein-induced and choline-deficient ethionine-supplemented (CDE) diet-induced acute pancreatitis. We found that there were significant differences in susceptibility to acute pancreatitis among mouse strains, and that susceptibility to acute pancreatitis was negatively or positively related with expression levels of Spink3 or Prss1, respectively. In addition, sequence differences in Spink3 promoter regions between JF1 and other strains were considered to be involved in differences in expression levels.

MATERIALS AND METHODS

Mouse Strains

All procedures were approved by the Animal Care and Use Committee of Kumamoto University. The five mouse strains were used in the following experiments: JF1 (Riken BioResource Center, Tsukuba, Japan), C57BL/6J, CBA/J, and BALB/c (CLEA Japan, Inc. Tokyo, Japan), and C3H/HeJ (Charles River Laboratories Japan, Inc. Yokohama, Japan). For every experiment, five mice in each strain were assigned to either a control or experimental group.

Cerulein-Induced Pancreatitis

After an overnight fast, mice were given hourly intraperitoneal injections of either saline (control) or cerulein (50 μg/kg) (Sigma-Aldrich Corp, Tokyo, Japan) for 12 h. One hour after the last injection, serum and the pancreas were isolated for the following studies.

CDE Diet-Induced Pancreatitis

Composition of CDE chow was described earlier.[28] Mice were fasted for 24 h and then fed with either CDE or control (regular laboratory chow) diet for 72 h. Then, animals were fed with regular laboratory chow for 12 h before they were killed.

Histological Examination and Pathologic Scoring

For histological analysis, pancreatic tissue was fixed overnight in 10% formalin, embedded in paraffin, sectioned, and stained with hematoxylin and eosin. The extent of injury was estimated using a method described earlier with some minor modifications.[29] Briefly, 10 randomly chosen microscopic fields were examined for each pancreas specimen, and the total surface of the slide was scored for five different variables determining severity of inflammation: edema (E), hemorrhage (H), inflammatory cell infiltration (I), acinar cell vacuolization (V), and acinar cell necrosis (N). Total scores for these five parameters were obtained in each group after mapping the pancreas into 10 fields and evaluating each field independently.

Serum Amylase Activity

Mouse blood was used to measure pancreatic amylase activity using substrate, 2-chloro-4-nitrophenyl-4-galactopyranosylmaltoside (Gal-G2-CNP) (CicaLiquid-N p-AMY, Kanto Chemical Co., Inc. Tokyo, Japan).

Measurement of Trypsin Activity

Measurement of trypsin activity was performed as described earlier.[25]

Northern Blot Analysis

Total RNAs were extracted from the pancreas with Sepasol (Nacalai Tesque, Kyoto, Japan). For making digoxigenin-labeled RNA probes (Roche Molecular Biochemicals, Germany), mouse Spink3 and Prss1 probes were derived from mouse pancreas RNA by reverse transcriptase PCR using the following nucleotide sequences: mPsti1 (agttcttctggcttttgcaccc) and mPsti26 (cccacgttgcctttcattacgg); Prss1: mPrss1-s1 (taaaggcaggcttccatccagg) and mPrss1-a1 (tgacagtgactgcagagggatt). cDNA was subsequently subcloned into a pGEM-T easy vector (Promega, Madison, WI, USA).

Sequence Analysis

Both cDNAs and the promoter regions of Spink3 and Prss1 gene were amplified by PCR using TaKaRa LA Taq polymerase mix (Takara Bio Inc., Kyoto, Japan). Primers used in the RT–PCR included the following sequences: mPsti1 (agttcttctggcttttgcaccc) and mPsti26 (cccacgttgcctttcattacgg) for Spink3; mPrss1-s1 (taaaggcaggcttccatccagg) and mPrss1-a1 (tgacagtgactgcagagggatt) for Prss1. Three pairs of primers were applied to sequence the 3 kb promoter region of each gene. Sequencing was performed using the Big Dye Terminator Cycle Sequencing ready kit and an ABI 310 Genetic Analyzer (Applied Biosystems).

Western Blot Analysis

Western blot analysis was carried out according to the method described earlier.[25] Primary antibodies to the following antigens were used at the indicated dilutions: Spink3 (Transgenic Inc., Kumamoto, Japan), 1:1000; Prss1 (Nordic immunological laboratories, Tilburg, Netherlands), 1:1000; amylase (Santa Cruz Biotechnology, CA, USA), 1:1000; and light chain 3 (LC3) (MBL International, Woburn, MA, USA),

1:1000. An anti-rabbit secondary immunoglobulin G antibody conjugated with horseradish peroxidase (Amersham Biosciences Corp, Piscataway, NJ, USA) was used to detect all proteins. Intensities of the bands were quantified by densitometry using ImageJ software (version 1.38, a program inspired by NIH image; http://rsb.info.nih.gov/ij/docs/index.html).

Statistical Analysis

All values are presented as mean ± s.d. (range, 95% CI), and statistical analysis was performed applying unpaired Student's *t*-tests. $P<0.05$ was considered to be a statistically significant difference.

RESULTS

Cerulein-Induced Pancreatitis

The pancreas of all strains of mice injected with normal saline showed no histological changes, whereas cerulein treatment induced variable degrees of acute pancreatitis among these five strains (Figure 1). C57BL/6J mice showed the mildest pancreatitis (Figure 1g and h), whereas C3H/HeJ mice displayed the most severe pancreatitis (Figure 1s and t). BALB/c and CBA/J mice showed a moderate degree of pancreatitis (Figure 1k, l, o and p). Acute pancreatitis in JF1 mice was obviously milder than pancreatitis in BALB/c and CBA/J mice, yet more severe than C57BL/6J with evidence of acinar cell necrosis (Figure 1c). Further calculations of semi-quantitative pathologic scores and statistical analysis strongly supported this statistical difference in susceptibility (Figure 1u and v). Levels of amylase coincide with histological findings, highest in C3H/HeJ, followed by CBA/J and BALB/c, and lowest in C57BL/6J and JF1 with statistically significant differences ($P<0.05$) (Figure 1w). Interestingly, serum levels of amylase in JF1 mice were lowest in spite of the presence of low grade of acinar cell necrosis when compared with C57BL/6J mice.

CDE Diet-Induced Pancreatitis

In CDE diet-induced pancreatitis, the general histological appearance of pancreatic tissues was much milder than those in cerulein-induced pancreatitis. Acinar cells presented almost no obvious histological changes in JF1, C57BL/6J or BALB/c mice (Figure 2c, d, g, h, k and l). C3H/HeJ mice, however, showed signs of obvious necrosis in acinar cells together with infiltration of inflammatory cells and slight vacuolization of acinar cells (Figure 2s and t). A mild degree of acinar cell necrosis was observed in CBA/J mice (Figure 2o and p). Peripancreatic hemorrhage was a frequent sign observed in this model as shown in Figure 2l, whereas fewer inflammatory cells were found within the pancreatic interstitium (Figure 2s). Pathologic scores were quite consistent to the microscopically gross observation (Figure 2u and w). Levels of serum amylase were proportional to these histological findings (Figure 2w).

Basal Expression Levels of Spink3 in Mice under Normal Feeding

Basal expression levels of Spink3 without induction were examined by western blot analysis in each strain of mice. Interestingly, results showed that expression of Spink3 was statistically higher in JF1 and C57BL/6J than the other three strains of mice that were susceptible to pancreatitis (Supplementary Figure 1).

Expression of Spink3 and Prss1 after Treatment with Cerulein

We examined the levels of mRNA and protein expressions of Spink3 and Prss1 without and with cerulein treatment. Without induction, CBA/J mice had lower Spink3 mRNA levels than those in other strains (Figure 3a and b). With cerulein treatment, Spink3 mRNA expression significantly increased in JF1, mildly in C57BL/6J, but decreased in BALB/c and C3H/HeJ strains (Figure 3a and c).

Without cerulein treatment, BALB/c mice had higher Prss1 mRNA levels than those in other strains (Figure 3a and b). After cerulein treatment, Prss1 mRNA levels in JF1, C57BL/6J, and BALB/c remained unchanged, but decreased in CBA/J and C3H/HeJ mice (Figure 3a and c). Expression G3PDH was notably augmented with cerulein treatment (Figure 3a), suggesting that this gene expression could not be used as reference loading control. Thus, we used 18S or 28S rRNA as reference RNAs.

Then, protein expression for Spink3 and Prss1 was examined by western blot analyses. Notably, Spink3 levels in JF1 mice decreased after overnight starvation (Figure 3e) when compared with normal feeding (see Supplementary Figure 1), although levels in other strains were unchanged after starvation. Without treatment, levels of Spink3 in C57BL/6J mice were higher than those in the other four strains (Figure 3d and e). With cerulein treatment, Spink3 expression was increased significantly in JF1, moderately in C57BL/6J and BALB/c, and slightly in CBA/J and C3H/HeJ (Figure 3d and f).

The level of Prss1 protein expression was lower in CBA/J and C3H/HeJ than those in the other three strains without induction (Figure 3d and e). However, levels of Prss1 increased significantly in BALB/c, CBA/J, and C3H/HeJ with cerulein treatment, whereas no notable changes were observed in JF1 and C57BL/6 strains (Figure 3d and f). Taken together, these results suggest that induction levels of Spink3 and Prss1 were negatively and positively related to susceptibility of cerulein-induced pancreatitis, respectively.

Expression of Spink3 and Prss1 with CDE Diet

When given a normal diet, levels of Spink3 mRNA in C57BL/6, CBA/J, and C3H/HeJ mice were higher than those in JF1 and BALB/c (Figure 4a and b). In the CDE diet model, Spink3 mRNA expression was significantly increased in JF1 mice, but mildly increased in C57BL/6J and CBA/J (Figure 4a and c).

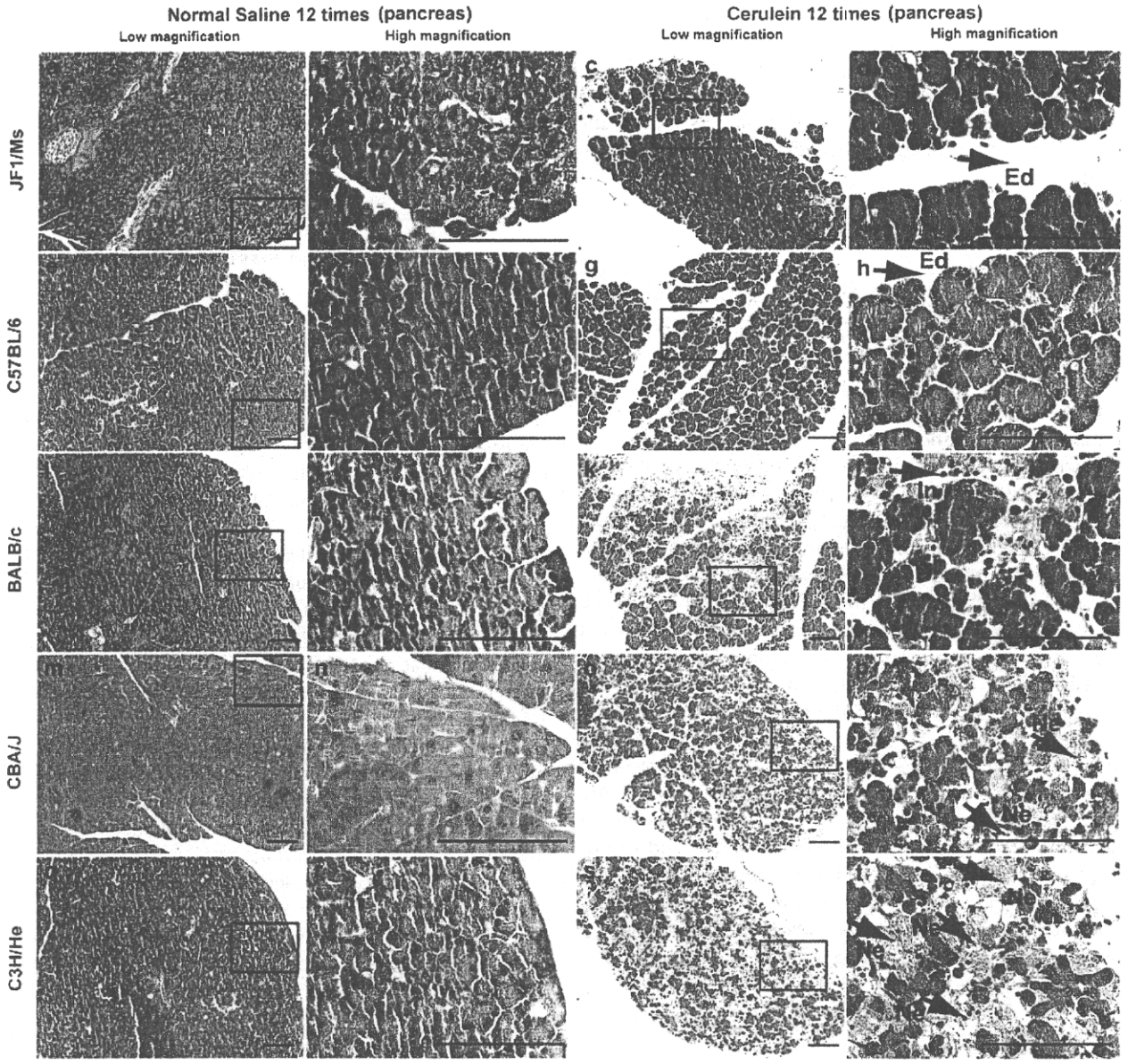

u Pathologic Scores in Cerulein-induced acute pancreatitis

M. Strain	Treat	No. of Mice	E	H	I	V	N	Total Scores	Mean ± SD
JF1/Ms	Saline	5	2	0	0	0	0	2	0.2 ± 0.12
	Cerulein	5	5	0	3	1	3	12	2.28 ± 0.49
C57BL/6	Saline	5	0	0	0	0	0	0	0.2 ± 0.12
	Cerulein	5	2	0	0	0	0	2	0.36 ± 0.11
BALB/c	Saline	5	0	0	0	0	0	0	0 ± 0
	Cerulein	5	4	0	4	3	7	18	3.6 ± 0.4
CBA/J	Saline	5	1	0	0	0	0	1	0.2 ± 0.18
	Cerulein	5	5	2	7	3	12	29	5.8 ± 1.02
C3H/He	Saline	5	2	0	0	0	0	2	0.2 ± 0.07
	Cerulein	5	7	1	9	1	20	38	7.6 ± 0.8

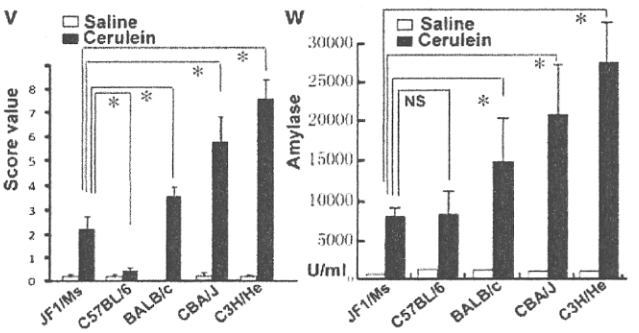

Figure 1 Histological changes, pathologic scores, and serum amylase levels in pancreas with and without cerulein treatment. (**a, b, e, f, i, j, m, n, q, r**) Saline-treated mice. (**c, d, g, h, k, l, o, p, s, t**) Cerulein-treated mice. (**b, d, f, h, j, l, n, p, r, t**) Higher magnification of areas indicated in (**a, c, e, g, i, k, m, o, q, s**). (**u**) Pathologic scores calculated based on five parameters: edema (E), hemorrhage (H), infiltrates (I), vacuolization (V), necrosis (N) of acinar cells. (**t**) Scores: total scores derived from the evaluation of five parameters. (**v**) Column graph of pathologic scores shown as mean ± s.d. (error bar). (**w**) Serum amylase levels. Black arrows indicate respective inflammatory changes. Scale bar: 50 μm. *$P<0.05$. NS: no significance.

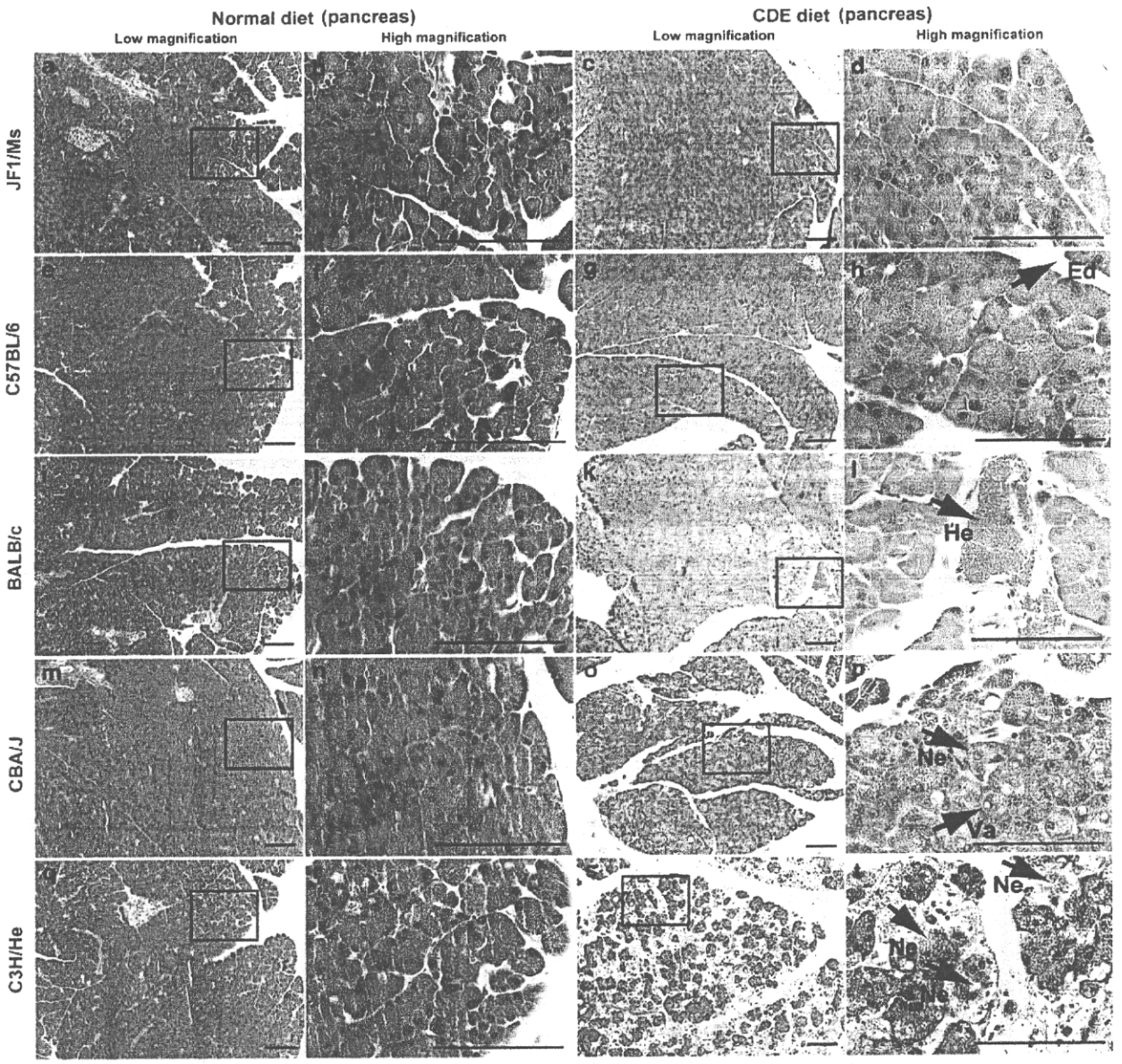

u Pathologic scores in CDE-diet acute pancreatitis

M. Strain	Treat	No. of Mice	E	H	I	V	N	Total Scores	Mean ± SD
JF1/Ms	N. Diet	5	2	1	0	0	0	3	0.6 ± 0.24
	CDE	5	2	2	0	3	0	7	1.4 ± 0.54
C57BL/6	N. Diet	5	1	0	0	0	0	1	0.2 ± 0.07
	CDE	5	3	0	0	2	0	5	1.0 ± 0.38
BALB/c	N. Diet	5	1	0	0	1	0	2	0.4 ± 0.57
	CDE	5	2	6	0	0	0	8	1.6 ± 0.32
CBA/J	N. Diet	5	2	0	0	0	0	2	0.4 ± 0.18
	CDE	5	3	3	0	1	5	12	2.4 ± 0.42
C3H/He	N. Diet	5	2	0	0	0	0	2	0.4 ± 0.2
	CDE	5	7	6	2	0	19	34	6.8 ± 1.40

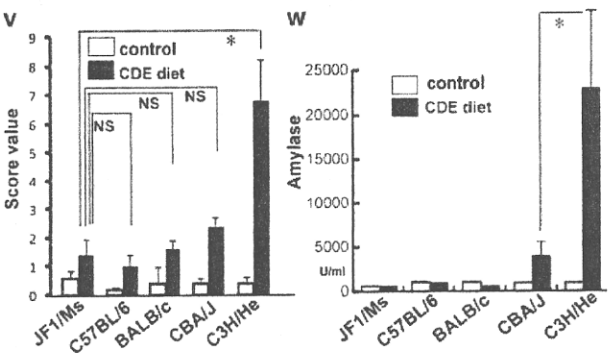

Figure 2 Histological changes, pathologic scores, and serum amylase levels in pancreas with and without CDE diet-induced acute pancreatitis. (**a, b, e, f, i, j, m, n, q, r**) Saline-treated mice. (**c, d, g, h, k, l, o, p, s, t**) Cerulein-treated mice. (**b, d, f, h, j, l, n, p, r, t**) Higher magnification of areas indicated in (**a, c, e, g, i, k, m, o, q, s**). (**u**) Pathologic scores calculated based on five parameters: edema (E), hemorrhage (H), infiltrates (I), vacuolization (V), necrosis (N) of acinar cells. (**v**) Column graph of the pathologic scores shown as mean ± s.d. (error bar). (**w**) Serum amylase levels. Black arrows indicate respective inflammatory changes. Scale bar: 50 μm. *$P<0.05$. NS: no significance.

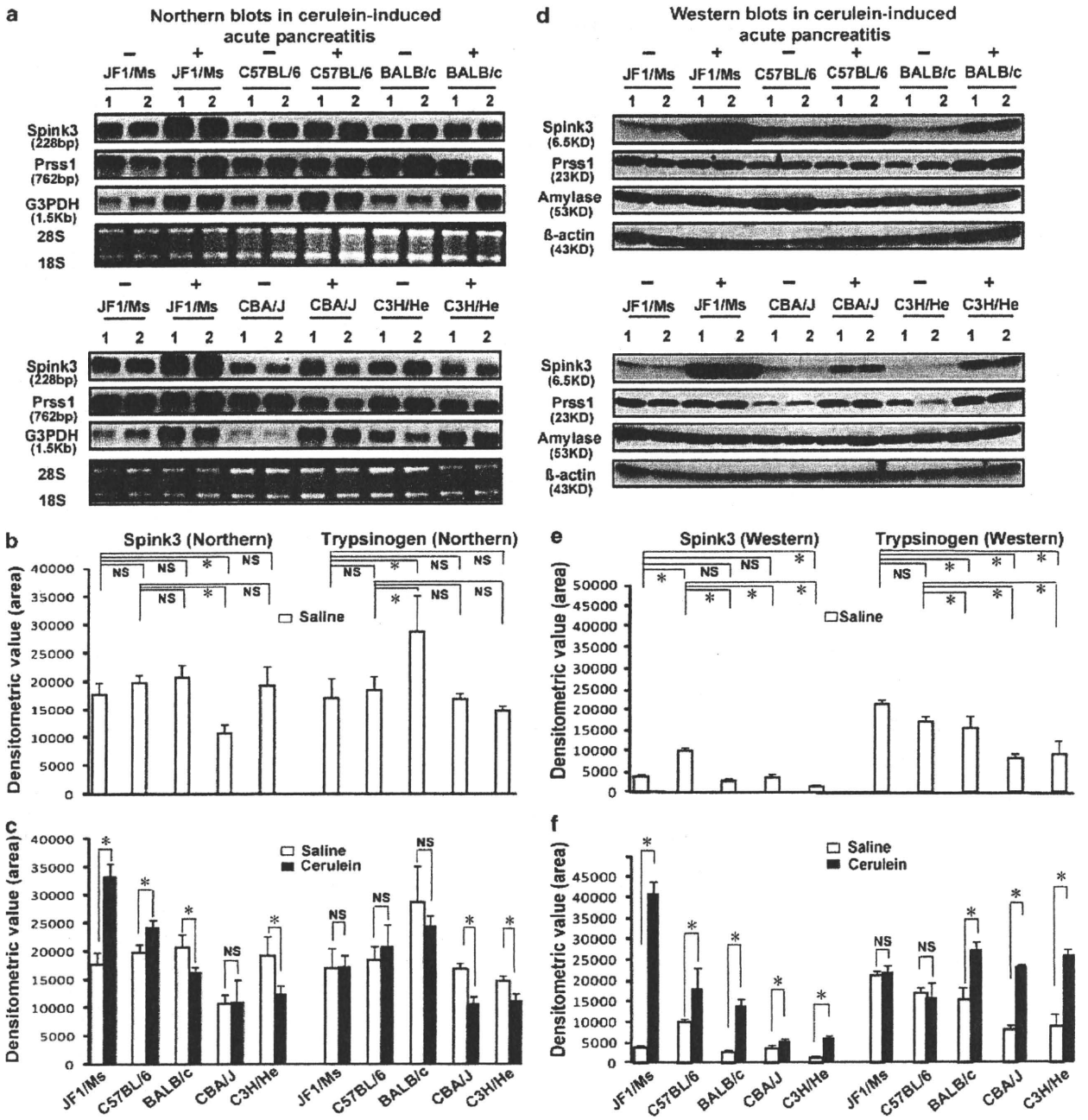

Figure 3 Northern and western blots analyses on Spink3, Prss1, and amylase expressions in cerulein-induced acute pancreatitis. (**a**) Northern blot analysis; 18S and 28S were used as loading controls because G3PDH expression was induced by cerulein treatment. The same JF1 samples were arranged in the first four lanes of northern blots. (**b**) Densitometric analysis for Spink3 and Prss1 expressions without cerulein induction in northern blot. (**c**) Densitometric analysis for Spink3 and Prss1 expressions with cerulein induction in northern blot. (**d**) Western blot analysis. β-actin was used as a loading control. The same JF1 samples were arranged in the first four lanes of western blots. (**e**) Densitometric analysis for Spink3 and Prss1 expressions after cerulein induction in western blot. (**f**) Densitometric analysis for Spink3 and Prss1 expressions with cerulein induction in western blot. Unfilled bars represent untreated strains of mice, whereas black bars indicate the treated strains. '−': saline treatment. '+': cerulein treatment. $^*P<0.05$. NS: no significance.

Levels of Prss1 mRNA in JF1 and C57BL/6 strains were lower than those in other strains under a normal diet (Figure 5a and b). After CDE diet, levels of Prss1 mRNA were decreased in C57BL/6, BALB/c, CBA/J, and C3H/HeJ mice (Figure 4a and c). Protein expression for Spink3 and Prss1 was examined by western blot analyses. Under normal diet, the levels of Spink3 were again higher in JF1 and C57BL/6J than those in other three strains (Figure 4d and e). After CDE

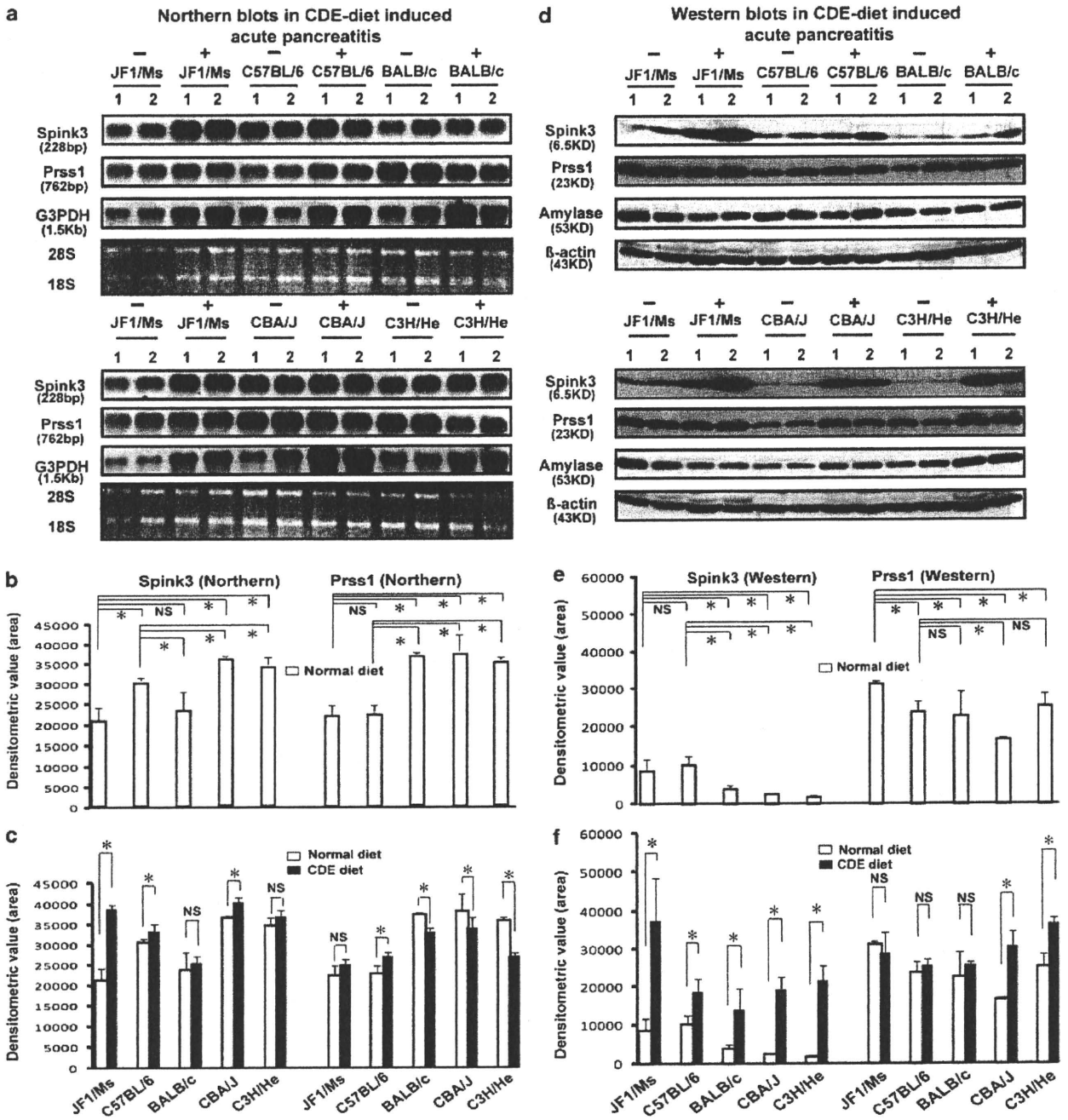

Figure 4 Northern and western blot analyses on Spink3, Prss1, and amylase expressions in CDE diet-induced acute pancreatitis. (**a**) Northern blot analysis; 18S and 28S were used as loading controls because G3PDH expression was induced by cerulein treatment. The same JF1 samples were arranged in the first four lanes of northern blots. (**b**) Densitometric analysis for Spink3 and Prss1 expressions without CDE diet in northern blot. (**c**) Densitometric analysis for Spink3 and Prss1 expressions with CDE diet in northern blot. (**d**) Western blot analysis. β-actin was used as a loading control. The same JF1 samples were arranged in the first four lanes of western blots. (**e**) Densitometric analysis for Spink3 and Prss1 expressions without CDE diet in western blot. (**f**) Densitometric analysis for Spink3 and Prss1 expressions with CDE diet in western blot. Unfilled bars represent untreated strains of mice, whereas black bars indicate the treated strains. *$P<0.05$. NS: no significance.

diet, Spink3 expression increased significantly in JF1, but moderately in other strains (Figure 4d and f).

The level of Prss1 protein expression was lower in CBA/J than those in other four strains without CDE diet (Figure 4d and e). With CDE diet, Prss1 expression increased significantly in CBA/J and C3H/HeJ, whereas expression remained unchanged in JF1, C57BL/6J, and BALB/c mice (Figure 4d and f). These results also suggest that the induction levels of Spink3 and Prss1 are negatively and positively related to susceptibility of CDE-induced pancreatitis, respectively.

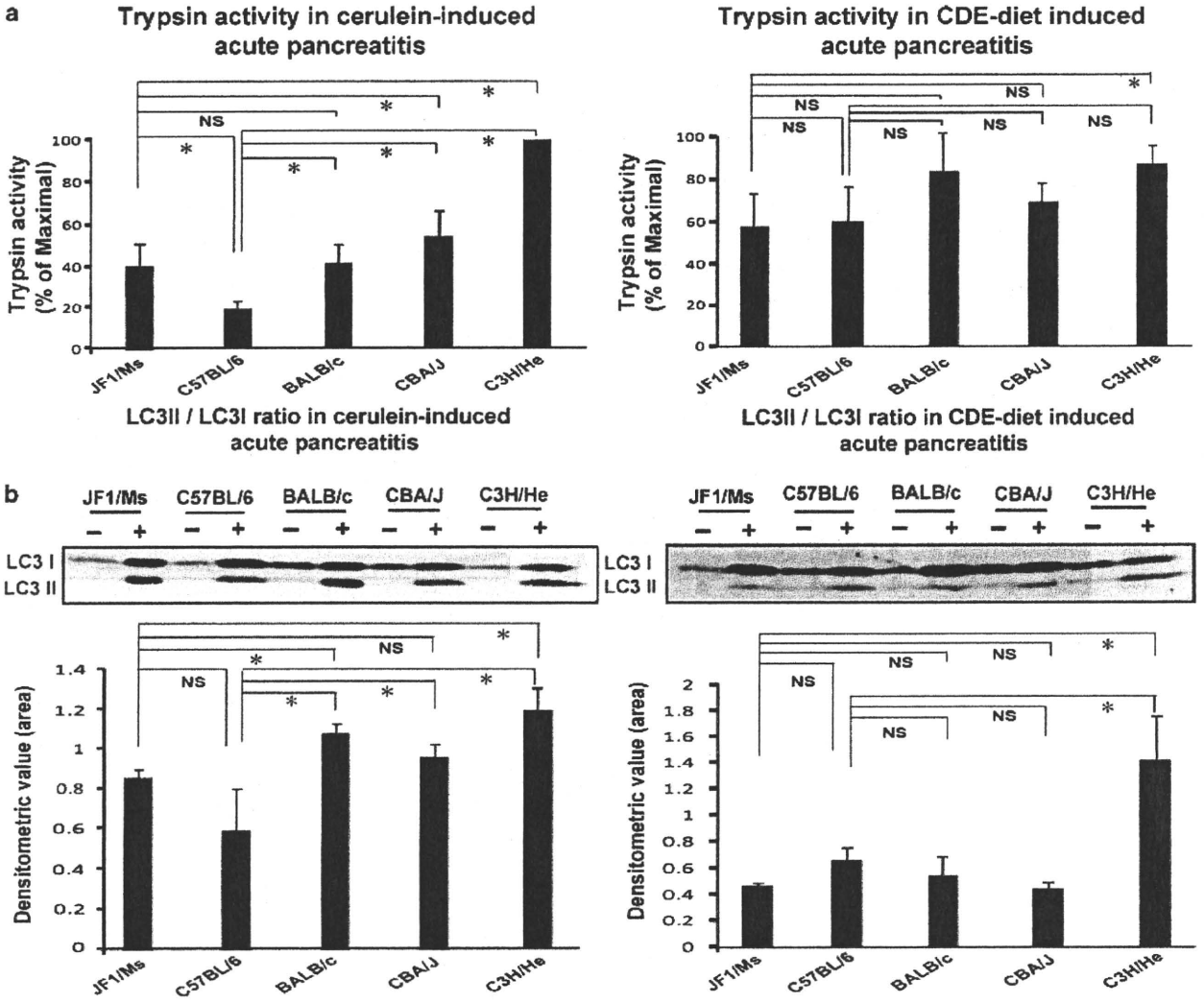

Figure 5 Trypsin activity and LC3-II expression. (**a**) Trypsin activity in cerulein-induced and CDE-diet-induced acute pancreatitis. Trypsin activity coincided with protein expression level of Prss1. (**b**) LC3-II/LC3-I ratio in cerulein-induced and CDE diet-induced acute pancreatitis. LC3-II levels were inversely related to Spink3 levels when treated with cerulein, suggesting the function of Spink3 as an inhibitor of autophagy.

Trypsin Activity

As activation or extent of trypsinogen to trypsin during initiation of acute pancreatitis is associated with the severity of acinar cell injury, we examined the trypsin activity level within pancreatic tissue homogenates among five mouse strains. The highest activity was shown in C3H/HeJ, followed by CBA/J, BALB/c, JF1, whereas C57BL/6J displayed the lowest value in cerulein-induced pacreatitis (Figure 5a, left panel). In CDE diet, trypsin activity level was significantly higher in C3H/HeJ than those in other strains (Figure 5a, right panel). Not surprisingly, the variation of trypsin activity was consistent with the expression pattern of trypsinogen among the five mouse strains.

Expression of LC3, an Autophagic Indicator

To approve that Spink3 functions also as a suppressor of autophagy, we checked in the five mouse strains the expression level of microtubule-associated protein 1 LC3. As LC3-I is converted into LC3-II during autophagosome formation, we determined the LC3-II/LC3-I ratio by densitometric analysis. As shown in Figure 5b, the ratio was higher in C3H/HeJ, BALB/c, and CBA/J than that in JF1 and C57BL/6J when treated with cerulein, showing that the mouse strain with higher Spink3 expression possessed low level of LC3-II, meaning less severe degree of autophagy.

Nucleotide Sequences of Prss1 and Spink3 cDNAs

To examine whether there was any nucleotide changes in coding regions of the *Prss1* and *Spink3* genes, we sequenced cDNA of these two genes isolated from all five strains. Nucleotide sequences of *Prss1* and *Spink3* cDNAs were exactly the same in four strains of mice: C57BL/6J, CBA/J, BALB/c, and C3H/HeJ. In contrast, in the 807 bp of the Prss1

Table 1 Single-nucleotide polymorphisms in JF1 cDNA *vs* B6

Prss1 (807 bp)			Spink3 (284 bp)		
Position	Nucleotide change	Amino-acid change	Position	Nucleotide change	Amino-acid change
Exon 1	15G>C	No	Exon 3	192G>A	No
Exon 3	342A>T	No	Exon 3	198C>T	No
Exon 4	516G>A	No	Exon 4	279A>G	No
Exon 4	519T>C	No			
Exon 4	568G>A	E190K			

JF1, Japanese Fancy Mouse 1. E190A, substitution of the glutamic acid (E) at amino-acid position 190 with lysine (K).

cDNA sequence of JF1 mice, five nucleotide changes were found (Table 1). However, only the alteration, G to A at position 568, resulted in substitution of glutamic acid with lysine at amino-acid position 190 (Table 1). On the other hand, three nucleotide changes were found within the 284 bp region of Spink3 cDNA of JF1 mice without an amino-acid substitution (Table 1).

Nucleotide Sequences of 3 kb Upstream Regions of Spink3 and Prss1 Genes

As expression patterns of Spink3 and Prss1 differed among mouse strains, we sequenced the approximately 3 kb promoter regions of Spink3 and Prss1 genes. We chose JF1 and C3H/HeJ as representatives of resistant and susceptible mouse strains, respectively. As the most conserved binding sites for transcription factors in pancreas-specific genes reside within the 1 kb upstream region, we focused on the 3 kb upstream regions of both Spink3 and Prss1 genes in this study. All of the sequence data were aligned and compared with the corresponding public database for C57BL/6J mice. For the upstream nucleotide sequence of the Spink3 gene, eight nucleotide changes (8/3000 = 0.27%) were found in C3H/HeJ *vs* C57BL/6J, whereas 92 nucleotide changes (92/3000 = 3.07%) appeared in JF1 *vs* C57BL/6J mice, representing a huge difference in the 3 kb upstream of the transcription start site in JF1 mice (Supplementary Figure 2). Notably, almost half of nucleotide changes[30] were found within the 1 kb upstream region in JF1 (Supplementary Figure 2). Several conserved motifs for transcription factors[31–36] were found in the 3 kb upstream regions of Spink3 genes as summarized in Supplementary Figure 2. Interestingly, an additional 10 bp was found between −372 and −381 in JF1 mice, although a conserved motif has not been reported around this region.

With respect to the Prss1 gene, 46 (46/3000 = 1.53%) or 39 (39/3000 = 1.30%) nucleotide changes were identified in C3H/He or JF1 strains against C57BL/6J mice, respectively (Supplementary Figure 3). However, the region between −3000 and −2300 bp of C57BL/6J was the same as that of JF1, but not of C3H. On the other hand, the region between −2300 and −1 bp of C57BL/6J mice was similar to that of C3H mice. Three binding sites were found in the 1 kb upstream region of the Prss1 gene[31,37] (Supplementary Figure 3). All these sequences are identical in all strains except one nucleotide change at −192 of the binding site (ATCACCTGCT) for nuclear protein in JF1 mice.

DISCUSSION

In this study, we showed strain differences using two models of experimental acute pancreatitis and identified a negative and positive relationship regarding the expression levels of Spink3 and Prss1, respectively, in the susceptibility to experimental acute pancreatitis. In addition, we showed that sequence differences in the promoter region of the Spink3 gene was significant between JF1 and other laboratory mouse strains, suggesting that differences in gene regulation are connected to a susceptibility to induced acute pancreatitis.

Pathologically, there were qualitative differences between cerulein- and CDE diet-induced pancreatitis in addition to the severity of pancreatitis. In the CDE diet model, much more hemorrhagic legions were noticed, as has been reported before.[28] This difference may be caused by different induction mechanisms in the early stages of acute pancreatitis. Cerulein is a cholecystokinin analog that can stimulate pancreatic acinar cells to secrete digestive enzymes. In supramaximal stimulation by cerulein, secretory activity increases dramatically, but membrane recruitment is insufficient for a strong demand of zymogen granule membrane, resulting in an inhibition of exocytosis at the luminal plasma membrane. On the other hand, a more likely target of ethionine is phospholipid metabolism of membranes that are involved in the processes of intracellular transport and secretion of pancreatic enzymes. Feeding a choline-deficient diet potentiated the activity of ethionine, because a choline-deficient diet also induced changes in membrane phospholipids of cellular organelles.[38–40] Although the detailed mechanism for hemorrhagic lesions remains unclear, destruction of the elastic tissue of the intrapancreatic vessels may also occur in such a situation.

In two experimental models, we observed similar strain differences in disease susceptibility, which were most severe in C3H/HeJ and CBA/J strains, moderate in BALB/c mice,

and mildest in C57BL/6J and JF1 strains. In human beings, a relationship between the PRSS1 gene mutations and the onset of pancreatitis has been established by many investigations.[21,30,41,42] Thus, it is possible that differences in primary structure or expression of the Prss1 gene are responsible for strain differences. Although we found one single-nucleotide polymorphism (SNP) in exon 4 that resulted in substitution of glutamic acid with lysine at amino-acid position 190 in JF1 mice, this mutation was not observed in the PRSS1 gene of human patients, suggesting that the coding region of the Prss1 gene is not related to the susceptibility to pancreatitis among these strains.

Interestingly, Prss1 protein expression was obviously increased in BALB/c, CBA/J, and C3H/HeJ mice, but not in JF1 and C57BL/6J mice with cerulein treatment. This high Prss1 expression coincided with a high trypsin activity. Many nucleotide changes found in the 3 kb upstream region of the Prss1 gene among C57BL/6J, C3H/HeJ, and JF1 strains may be responsible for different expression level.

Differences in the primary structure or expression of the Spink3 gene may also be involved in susceptibility to the development of pancreatitis. However, we could not find any SNPs with an amino-acid substitution between JF1 and other strains of mice. Thus, the coding region of the Spink3 gene was not related to pancreatitis susceptibility. Meaningfully, we found a significantly higher expression of Spink3 in JF1 and C57BL/6J mice under normal feeding (Figure 3a and b). Furthermore, Spink3 expression was strongly augmented in JF1 mice with cerulein treatment. This high Spink3 expression was associated with low level of LC3-II expression, implying the function of Spink3 as an inhibitor of autophagy. As shown in Supplementary Figure 2, we found significant nucleotide changes in the 3 kb upstream region of the Spink3 gene of JF1 mice. It is of interest that an additional 10 bp was inserted between −372 and −381 region in JF1 mice, although a conserved motif has not been reported around this region. Therefore, this region might be involved in the regulation of gene expression under cerulein stimulation. Taking these into account, the mechanisms by which Prss1 and Spink3 might be influencing the susceptibility are proposed here in a molecular model shown in Figure 6. In resistant strains, increased Spink3 expression caused by cerulein or CDE diet suppresses autophagy, leading to reduced activation of trypsinogen. In addition, Spink3 can bind to trypsin to inhibit its activity directly. Thus, both enhanced Spink3 and low Prss1 expression result in reduced trypsin activity, leading to less severe acute pancreatitis. In susceptible strains, low level of Spink3 expression results in enhanced autophagy, causing the conversion of trypsinogen to trypsin, and in low-level inhibition of trypsin. Thus, both high Prss1 and low Spink3 expressions result in increased trypsin activity, leading to more severe acute pancreatitis.

After activation of trypsinogen, inflammation is eventually induced in both models. Therefore, different responses in inflammatory factors, such as NF-κB, TNF-α, IL-1,

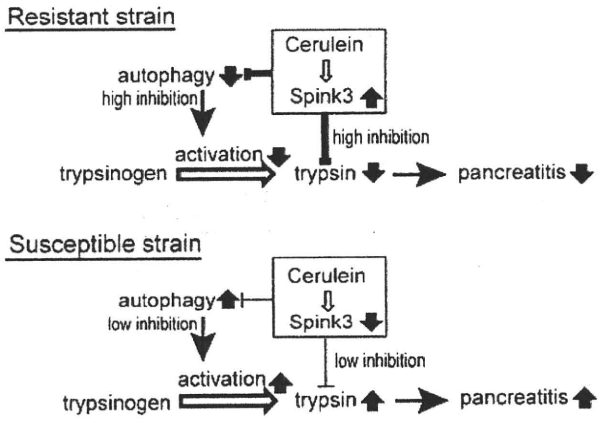

Figure 6 Proposed model for the function of Prss1 and/or Spink3 on susceptibility of acute pancreatitis. In resistant strains, increased Spink3 expression caused by cerulein suppresses autophagy, and trypsin activity, leading to less severe acute pancreatitis. In susceptible strains, low expression of Spink3 and high expression of Prss1 result in enhanced autophagy, causing the conversion of trypsinogen to trypsin and in low-level inhibition of trypsin, thus leading to more severe acute pancreatitis.

Heat Shock Protein, NO, or TLR4, among strains may be involved in pancreatitis susceptibility. Actually, inflammatory responses are different from one strain to another and a given strain can have variable inflammatory responses from one form of damage to another. For example, inbred mice varied significantly in their susceptibility to cigarette smoke-induced emphysema.[43,44] Further studies will be required to analyze genetic mechanisms for differences in inflammatory responses.

Advances in molecular physiology indicate the mouse to be an ideal investigative model to determine genomic variants that affect susceptibility to disease. This model offers the advantage of studying a large number of genetically identical animals under controlled conditions. Animal studies complement human studies by introducing an experimental control and the opportunity to pursue functional genomics and expression studies at the level of organs, tissues, or cells. Molecular mechanisms for disease resistance/susceptibility may differ among strains, and the JF1 strain may give a unique opportunity to examine such mechanisms that may not be found in other laboratory mouse strains.

Supplementary Information accompanies the paper on the Laboratory Investigation website (http://www.laboratoryinvestigation.org)

ACKNOWLEDGEMENTS

We herein sincerely appreciate the excellent work on the tissue sectioning preparation by Mrs Michiyo Nakata and Ms Yumi Otake. We also thank the Riken BioResource Center, Tsukuba, Japan for supplying JF1 mice. This work was supported in part by KAKENHI (Grant-in-Aid for Scientific Research) in Priority Areas 'Integrative Research Toward the Conquest of Cancer' (17012018) from the Ministry of Education, Culture, Sports, Science, and Technology, a Grant-in-Aid for Scientific Research (S) (21220010) and a Grant-in-Aid for Young Scientists (B) (18790968) from the Japan Society for the Promotion of Science (JSPS) of Japan.

DISCLOSURE/CONFLICT OF INTEREST
The authors declare no conflict of interest.

1. Beck JA, Lloyd S, Hafezparast M, *et al.* Genealogies of mouse inbred strains. Nat Genet 2000;24:23–25.
2. Moore KJ. Utilization of mouse models in the discovery of human disease genes. Drug Discov Today 1999;4:123–128.
3. Yonekawa H, Moriwaki K, Gotoh O, *et al.* Hybrid origin of Japanese mice 'Mus musculus molossinus': evidence from restriction analysis of mitochondrial DNA. Mol Biol Evol 1988;5:63–78.
4. Prager EM, Orrego C, Sage RD. Genetic variation and phylogeography of central Asian and other house mice, including a major new mitochondrial lineage in Yemen. Genetics 1998;150:835–861.
5. Wade CM, Kulbokas III EJ, Kirby AW, *et al.* The mosaic structure of variation in the laboratory mouse genome. Nature 2002;420:574–578.
6. Sakai T, Miura I, Yamada-Ishibashi S, *et al.* Update of mouse microsatellite database of Japan (MMDBJ). Exp Anim 2004;53:151–154.
7. Abe K, Noguchi H, Tagawa K, *et al.* Contribution of Asian mouse subspecies Mus musculus molossinus to genomic constitution of strain C57BL/6J, as defined by BAC-end sequence-SNP analysis. Genome Res 2004;14:2439–2447.
8. Jansa P, Divina P, Forejt J. Construction and characterization of a genomic BAC library for the Mus m. musculus mouse subspecies (PWD/Ph inbred strain). BMC Genomics 2005;6:161.
9. Moriwaki K. Wild mouse from geneticist's viewpoint. In: Moriwaki K, Shiroishi T, Yonekawa H (eds). Genetics in Wild Mice: Its Application to Biomedical Research. Japan Scientific Press/Karger: Tokyo, 1994, pp xiii–xxiv.
10. Koide T, Moriwaki K, Uchida K, *et al.* A new inbred strain JF1 established from Japanese fancy mouse carrying the classic piebald allele. Mamm Genome 1998;9:15–19.
11. Surwit RS, Kuhn CM, Cochrane C, *et al.* Diet-induced type II diabetes in C57BL/6J mice. Diabetes 1988;37:1163–1167.
12. Kobayashi M, Ohno T, Tsuchiya T, *et al.* Characterization of diabetes-related traits in MSM and JF1 mice on high-fat diet. J Nutr Biochem 2004;15:614–621.
13. Gukovskaya AS, Hosseini S, Satoh A, *et al.* Ethanol differentially regulates NF-kappaB activation in pancreatic acinar cells through calcium and protein kinase C pathways. Am J Physiol Gastrointest Liver Physiol 2004;286:G204–G213.
14. Pandol SJ. Acute pancreatitis. Curr Opin Gastroenterol 2005;21: 538–543.
15. Satoh A, Gukovskaya AS, Reeve Jr JR, *et al.* Ethanol sensitizes NF-kappaB activation in pancreatic acinar cells through effects on protein kinase C-epsilon. Am J Physiol Gastrointest Liver Physiol 2006;291:G432–G438.
16. Schenker S, Montalvo R. Alcohol and the pancreas. Recent Dev Alcohol 1998;14:41–65.
17. Acosta JM, Ledesma CL. Gallstone migration as a cause of acute pancreatitis. N Engl J Med 1974;290:484–487.
18. Lerch MM, Hernandez CA, Adler G. Gallstones and acute pancreatitis–mechanisms and mechanics. Dig Dis 1994;12:242–247.
19. Rosendahl J, Bodeker H, Mossner J, *et al.* Hereditary chronic pancreatitis. Orphanet J Rare Dis 2007;2:1.
20. Hirota M, Ohmuraya M, Baba H. Genetic background of pancreatitis. Postgrad Med J 2006;82:775–778.
21. Whitcomb DC, Gorry MC, Preston RA, *et al.* Hereditary pancreatitis is caused by a mutation in the cationic trypsinogen gene. Nat Genet 1996;14:141–145.
22. Varallyay E, Pal G, Patthy A, *et al.* Two mutations in rat trypsin confer resistance against autolysis. Biochem Biophys Res Commun 1998;243:56–60.
23. Witt H, Luck W, Hennies HC, *et al.* Mutations in the gene encoding the serine protease inhibitor, Kazal type 1 are associated with chronic pancreatitis. Nat Genet 2000;25:213–216.
24. Ohmuraya M, Hirota M, Araki K, *et al.* Enhanced trypsin activity in pancreatic acinar cells deficient for serine protease inhibitor kazal type 3. Pancreas 2006;33:104–106.
25. Hashimoto D, Ohmuraya M, Hirota M, *et al.* Involvement of autophagy in trypsinogen activation within the pancreatic acinar cells. J Cell Biol 2008;181:1065–1072.
26. Ohmuraya M, Yamamura K. Autophagy and acute pancreatitis: a novel autophagy theory for trypsinogen activation. Autophagy 2008;4: 1060–1062.
27. Rosendahl J, Witt H, Szmola R, *et al.* Chymotrypsin C (CTRC) variants that diminish activity or secretion are associated with chronic pancreatitis. Nat Genet 2008;40:78–82.
28. Lombardi B, Estes LW, Longnecker DS. Acute hemorrhagic pancreatitis (massive necrosis) with fat necrosis induced in mice by DL-ethionine fed with a choline-deficient diet. Am J Pathol 1975;79:465–480.
29. Schmidt J, Lewandrowski K, Fernandez-del Castillo C, *et al.* Histopathologic correlates of serum amylase activity in acute experimental pancreatitis. Dig Dis Sci 1992;37:1426–1433.
30. Nishimori I, Kamakura M, Fujikawa-Adachi K, *et al.* Mutations in exons 2 and 3 of the cationic trypsinogen gene in Japanese families with hereditary pancreatitis. Gut 1999;44:259–263.
31. Boulet AM, Erwin CR, Rutter WJ. Cell-specific enhancers in the rat exocrine pancreas. Proc Natl Acad Sci USA 1986;83:3599–3603.
32. Cockell M, Stevenson BJ, Strubin M, *et al.* Identification of a cell-specific DNA-binding activity that interacts with a transcriptional activator of genes expressed in the acinar pancreas. Mol Cell Biol 1989;9: 2464–2476.
33. Roux E, Strubin M, Hagenbuchle O, *et al.* The cell-specific transcription factor PTF1 contains two different subunits that interact with the DNA. Genes Dev 1989;3:1613–1624.
34. Stevenson BJ, Hagenbuchle O, Wellauer PK. Sequence organisation and transcriptional regulation of the mouse elastase II and trypsin genes. Nucleic Acids Res 1986;14:8307–8330.
35. Swift GH, Hammer RE, MacDonald RJ, *et al.* Tissue-specific expression of the rat pancreatic elastase I gene in transgenic mice. Cell 1984;38:639–646.
36. Yasuda T, Ohmachi Y, Katsuki M, *et al.* Identification of novel pancreas-specific regulatory sequences in the promoter region of human pancreatic secretory trypsin inhibitor gene. J Biol Chem 1998;273:34413–34421.
37. Howard G, Keller PR, Johnson TM, *et al.* Binding of a pancreatic nuclear protein is correlated with amylase enhancer activity. Nucleic Acids Res 1989;17:8185–8195.
38. Chen SH, Estes LW, Lombardi B. Lecithin depletion in hepatic microsomal membranes of rats fed on a choline-deficient diet. Exp Mol Pathol 1972;17:176–186.
39. Leelavathi DE, Katyal SL, Lombardi B. Lecithin depletion in liver mitochondria of rats fed a choline-deficient diet. Effect on beta-hydroxybutyrate dehydrogenase. Life Sci 1974;14:1203–1210.
40. Lombardi B. Effects of choline deficiency on rat hepatocytes. Fed Proc 1971;30:139–142.
41. Howes N, Greenhalf W, Stocken DD, *et al.* Cationic trypsinogen mutations and pancreatitis. Clin Lab Med 2005;25:39–59.
42. O'Reilly DA, Kingsnorth AN. Hereditary pancreatitis and mutations of the cationic trypsinogen gene. Br J Surg 2000;87:708–717.
43. Guerassimov A, Hoshino Y, Takubo Y, *et al.* The development of emphysema in cigarette smoke-exposed mice is strain dependent. Am J Respir Crit Care Med 2004;170:974–980.
44. Shapiro SD. Animal models for chronic obstructive pulmonary disease: age of klotho and marlboro mice. Am J Respir Cell Mol Biol 2000; 22:4–7.

Mod Rheumatol (2010) 20:222–232
DOI 10.1007/s10165-010-0279-5

ORIGINAL ARTICLE

Safety and efficacy profiles of tocilizumab monotherapy in Japanese patients with rheumatoid arthritis: meta-analysis of six initial trials and five long-term extensions

Norihiro Nishimoto · Kyoko Ito · Nobuhiro Takagi

Received: 9 December 2009 / Accepted: 26 January 2010 / Published online: 11 March 2010

Abstract We present safety and efficacy data from Japanese clinical studies on monotherapy with tocilizumab (TCZ), a humanized anti-interleukin 6 receptor monoclonal antibody, in which 601 patients with moderate to severe rheumatoid arthritis, with a total of 2188 patient-years (pt-yr) exposure, were enrolled. The median treatment duration was 3.8 years. The incidence of adverse events (AEs), including abnormal laboratory test results, was calculated as 465.1 per 100 pt-yr. The most common serious adverse events (SAEs) were infections (6.22 per 100 pt-yr). There was no increase in the frequency of AEs or SAEs with long-term treatment. Abnormalities in the laboratory test results, such as increases in lipid parameters or abnormal liver function parameters, were common, but most were mild and there were no SAEs related to them. At baseline, 546 patients (90.8%) were taking corticosteroids; of these, 77.8% were able to decrease their corticosteroid dose during the study period, while 35.2% discontinued corticosteroids altogether. In the patients treated longer than 5 years, 91.3, 73.0, and 51.3% met the ACR20, ACR50, and ACR70 response criteria, respectively, and 59.7% met the DAS remission criterion (DAS28 <2.6) at 5 years. In conclusion, based on these results, TCZ has shown good tolerability and high efficacy during long-term treatment.

Keywords Clinical trial · Interleukin-6 · Meta-analysis · Rheumatoid arthritis · Tocilizumab

N. Nishimoto
Wakayama Medical University, 811-1 Kimiidera, Wakayama, Wakayama 641-8509, Japan

K. Ito · N. Takagi
Chugai Pharmaceutical Co., Ltd., 1-1 Nihonbashi-Muromachi 2-chome, Chuo-ku, Tokyo 103-8324, Japan

N. Nishimoto (✉)
Laboratory of Immune Regulation, Wakayama Medical University, 7-7-20 Saito-Asagi, Ibaraki, Osaka 567-0085, Japan
e-mail: norichan@wakayama-med.ac.jp

Introduction

Rheumatoid arthritis (RA) is a common autoimmune disease characterized by persistent synovitis and progressive destruction of cartilage and bone in multiple joints [1]. The affected joints exhibit hyperplasia of inflamed synovium infiltrated with a range of immune cells; the inflamed synovium in turn forms pannus tissue that invades cartilage and bone [2]. Interleukin 6 (IL-6) is a multifunctional cytokine produced by various cell types, including T cells, B cells, monocytes, fibroblasts, and endothelial cells. It binds to membrane-expressed or soluble IL-6 receptors (IL-6R), and the resulting IL-6/IL-6R complex then binds to gp130, a common signal transduction molecule for cytokines of the IL-6 family, resulting in signal transduction to the cell nucleus [3]. Most of the clinical abnormalities seen in RA can be explained in terms of the dysregulated hyperproduction of IL-6. High levels of IL-6 are present in synovial fluid from affected joints of patients with active RA, and the IL-6 level correlates with the degree of radiological joint damage [4, 5].

Tocilizumab (TCZ) is a humanized anti-human IL-6R monoclonal antibody that inhibits IL-6 binding to IL-6R [6]. It was humanized by grafting the complementarity-determining regions from a murine anti-IL-6R antibody into human immunoglobulin (Ig) G1, thereby creating a functioning antigen-binding site in a reshaped human antibody and reducing the antigenicity of the antibody in

humans. We have demonstrated that treatment with TCZ improves the signs and symptoms of RA and also prevents joint damage [7–11]. TCZ has been developed as an anti-rheumatic agent. It was first approved in Japan in April 2008 and in the European Union in January 2009. Many other countries, including Brazil and India, have also approved its use in the clinical setting.

Here we present our meta-analysis of long-term safety and efficacy data from Japanese clinical studies of TCZ in patients with disease-modifying antirheumatic drugs (DMARD)-refractory RA.

Patients and methods

Patients

The eligibility criteria and study design for each study have already been reported [7–11]. Briefly, eligible patients were ≥20 years of age and fulfilled the 1987 American Rheumatism Association criteria for RA [12] with a disease history of >6 months (with the exception of the SAMURAI study, in which the eligible disease duration was restricted to between 0.5 and 5 years). All subjects failed to respond satisfactorily to treatment with at least one DMARD, including methotrexate (MTX) or immunosuppressants. At enrollment in the initial trials, the patients had active RA, as defined as the presence of six or more swollen joints, and tender joints. Patients receiving steroids (≤10 mg/day as prednisolone) and/or non-steroidal anti-inflammatory drugs (NSAIDs) were eligible if the dose had not increased during the 1-month washout period. Sexually active premenopausal women were required to have a negative urine pregnancy test at entry and periodically thereafter and to use effective contraception during the study period. There was no requirement to screen patients for exposure to tuberculosis (TB) or to have a Mantoux test before enrollment; the prophylactic use of anti-TB drugs was also not required.

Study protocols

We report here our meta-analysis of six clinical studies of TCZ in RA, all of which were conducted in Japan, and their five uncontrolled long-term extensions. The patient population for this meta-analysis consisted of all those individuals who received at least one dose of TCZ within the framework of the six clinical studies and/or extension studies. The initial clinical studies examined in this meta-analysis were a phase I/II open-label dose escalation study [7], a phase II double-blind dose finding study [8], a phase III open-label randomized study (SAMURAI) [9], a phase III double-blind study (SATORI) [10], a drug–drug interaction study, and a renal failure study (Fig. 1). All study protocols were approved by the Ministry of Health, Labor and Welfare of Japan and by the Ethics Committee of each institute, and the patients all gave their written informed consent. All patients received either placebo or 2, 4, or 8 mg/kg body weight of TCZ in the initial study and 8 mg/kg body weight of TCZ in the extension study. Patients receiving a corticosteroid dose of ≤10 mg/day (as prednisolone) at entry to the initial study were permitted to continue corticosteroid treatment. Surgical treatment and concomitant use of NSAIDs and corticosteroids was allowed, but concomitant use of DMARDs and immunosuppressive treatments was excluded.

Serious adverse events (SAEs) were defined as AEs that were fatal or life-threatening, resulting in permanent or significant disability or requiring prolonged inpatient hospitalization. SAEs and AEs were classified, using MedDRA (Medical Dictionary for Regulatory Activities) ver. 8.0 (published by the Maintenance and Support Services Organization). Any abnormality in laboratory test results was graded by the common terminology criteria for AEs ver. 3.0 (National Cancer Institute, Bethesda, MD).

Clinical response was measured using the American College of Rheumatology (ACR) response criteria, the Disease Activity Score in 28 joints (DAS28), and the DAS28-based European League against Rheumatism (EULAR) criteria. Remission was defined, in accordance with the EULAR definition, as DAS28 <2.6 [13]. Functional disability was self-assessed by patients using the modified Health Assessment Questionnaire (mHAQ).

Statistical analysis

All data from the first dosing of TCZ to the last observation time for each patient were analyzed. Where appropriate, initial study data were combined with extension study data (matching on patient number). No imputation or estimation methods were used for missing data during the study.

The baseline time point for patient demographics, disease history, exposure, and AEs was the time of the first received dose of TCZ, which was either at the first dose in the initial controlled study or the first dose in the extension study. A Kaplan–Meier plot displaying time to withdrawal was produced. Patients were censored at the data cut-off time (if they had not already withdrawn). Data on AEs were summarized as the number of incidents per 100 patient-years (pt-yr).

A paired *t* test was used to detect statistically significant differences in disease activity and functional disability compared to baseline. Statistical analyses were performed using SAS ver. 8.2 TS2M0 (SAS Institute, Cary, NC).

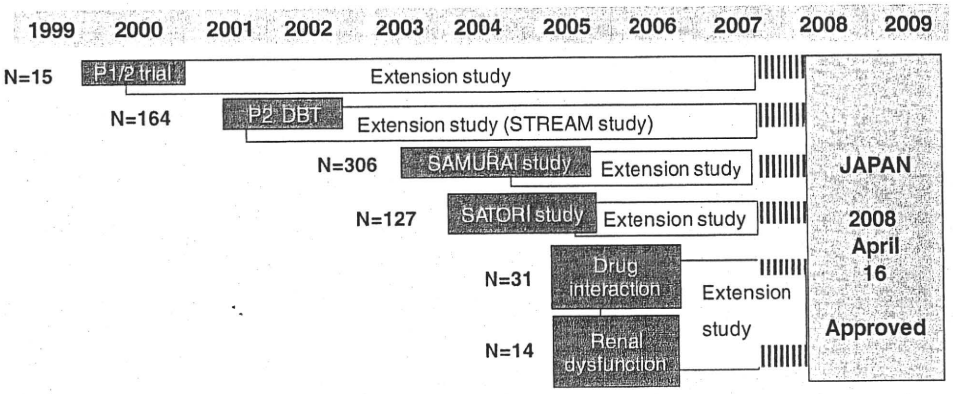

Fig. 1 Overview of clinical studies of tocilizumab (TCZ) in Japan. In total, 657 patients were enrolled in the initial studies and 601 patients received TCZ in the initial studies or the extensions. *DBT* Double-blind trial

Results

Patient characteristics

In total, 657 RA patients were initially enrolled and 601 were ultimately treated (i.e., received at least one dose of TCZ) in the clinical trials surveyed here (Fig. 1). The 56 patients who were not treated had been enrolled in the placebo group in the controlled studies but withdrew before they were enrolled in the extension studies. The mean age of the treated patients at baseline was 53.1 years (range 21–80 years), 80.5% were women, and the mean duration of RA was 6.5 years (range 0.4–52.8 years). The mean number of DMARDs previously administered was 3.5; 485 patients (80.8%) had previously received MTX, and 542 (90.8%) were taking corticosteroids (prednisolone-equivalent dose: mean 6.7 mg/day, range 0–10 mg/day) (Table 1).

The median duration of TCZ treatment was 3.8 years (range 0.1–9.0 years), and the total exposure was 2188 pt-yr. Only 27.6 and 35.7% of the patients had withdrawn from these studies at the 3- and 5-year data cut-off time point, respectively (Fig. 2). Of the treated patients, 118 (19.6%) withdrew due to AEs. Only eight patients (1.3%) withdrew due to an unsatisfactory response.

Safety

All AEs and adverse drug reactions (ADRs, that is, AEs at least possibly related to TCZ) are summarized in Table 2 according to the MedDRA system organ class (SOC). There were 10,176 AEs in 596 (99.2%) of the 601 patients administered TCZ (465.1/100 pt-yr). There was no increase in the incidence of AEs with long-term treatment. The SOCs in which AEs occurred frequently (>30 events/100 pt-yr) were "infections and infestations", "investigations", "gastrointestinal disorders", and "skin and subcutaneous tissue disorders". Among the category

Table 1 Demographics and baseline clinical characteristics of rheumatoid arthritis patients who received tocilizumab in clinical studies in Japan

Demographics and baseline clinical characteristics	Value
Total patients treated with TCZ (*n*)	601
Total exposure (patient-years) (*n*)	2188
Demographics	
Age (years)	53.1 ± 11.4
Median (years, range)	54.0 (21–80)
Women (% of patients)	80.5
Body weight (kg)	54.2 ± 20.1
Clinical characteristics	
Duration of RA (years)	6.5 ± 7.1
Median duration (years)	4.1
Previous DMARDs (*n*)	3.5 ± 1.8
Previous biologics (%)	2.5
Concomitant oral steroid (% of patients)	90.8%
Dose (mg/day)	6.7 ± 2.5
RA stage[a] (%, at I/II/III/IV)	4.7/36.4/32.3/26.6
RA classification[b] (%, at I/II/III/IV)	8.2/72.2/19.6/0.0
Tender joint count, 0–49 joints	16.1 ± 9.2
Swollen joint count, 0–46 joints	12.9 ± 7.6
ESR (mm/h)	63.0 ± 30.6
CRP (mg/dL)	4.0 ± 3.0
DAS28	6.3 ± 1.0

Values are given as the mean ± standard deviation (SD) unless stated otherwise

Calculated from patient data at first infusion of active tocilizumab, i.e., baseline of the initial trial (TCZ groups) or extension (placebo group in initial trial)

DMARDs Disease-modifying antirheumatic drugs, *TCZ* tocilizumab, a humanized anti-interleukin-6 receptor antibody, *RA* rheumatoid arthritis, *ESR* erythrocyte sedimentation rate, *CRP* C-reactive protein, *DAS28* Disease Activity Score in 28 joints

[a] RA stage determined by Steinbrocker's criteria

[b] RA functional status determined by the American College of Rheumatology (ACR) response criteria

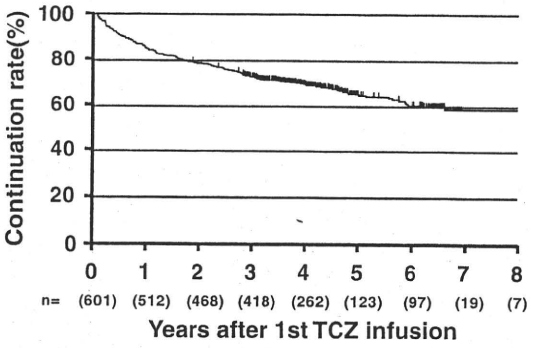

Fig. 2 The retention rate of patients treated with tocilizumab in the studies analyzed (Kaplan–Meier analysis). Treatment time was calculated from first infusion of TCZ at any dose, excluding time receiving placebo in an initial study. Patients are treated as a censored case if the patients finished a study with the completion of that study

"infections and infestations", the common AEs were upper respiratory infection, tinea, urinary tract infection, bronchitis, gastroenteritis, and pneumonia (Table 3).

In total, 133 infusion reactions were observed in 93 patients (15.5%), mostly within the first four infusions, among which headache, pruritus, and increased blood pressure were the most common. No patients were withdrawn due to infusion reactions. Anaphylaxis or anaphylactic reactions occurred in three patients; there were no serious infusion reactions due to the production of anti-TCZ antibodies.

There were 506 SAEs in 261 patients (23.1/100 pt-yr) and 223 serious ADRs in 133 patients (10.2/100 pt-yr) (Table 4). There were five deaths, giving a mortality rate of 0.23/100 pt-yr. The SOC with the most common SAEs was "infections and infestations" (6.22/100 pt-yr); this was followed by "musculoskeletal and connective tissue disorders" (5.53/100 pt-yr), which mostly related to joint surgery and were classified as unrelated to TCZ. Long-term exposure to TCZ did not increase the incidence of SAEs.

The common serious infections were pneumonia (28 events, 1.28/100 pt-yr), herpes zoster (14 events, 0.64/100 pt-yr), and cellulitis (13 events, 0.59/100 pt-yr). For

Table 2 Classification of adverse events and adverse drug reactions among patients receiving tocilizumab according to system organ class

SOC	Adverse events		Adverse drug reactions	
	Number of events	Events/ 100 patient-years	Number of events	Events/ 100 patient-years
Total	10176	465.1	6681	305.4
Infections and infestations	2696	129.2	2266	103.6
Neoplasms benign, malignant, and unspecified	61	2.78	41	1.87
Blood and lymphatic system disorders	56	2.56	32	1.46
Immune system disorders	64	2.93	32	1.46
Endocrine disorders	10	0.45	7	0.32
Metabolism and nutrition disorders	54	2.47	37	1.69
Psychiatric disorders	81	3.70	24	1.10
Nervous system disorders	463	21.2	295	13.5
Eye disorders	267	12.2	141	6.40
Ear and labyrinth disorders	68	3.10	32	1.46
Cardiac disorders	87	3.98	46	2.10
Vascular disorders	121	5.53	90	4.11
Respiratory, thoracic, and mediastinal disorders	511	23.4	400	18.3
Gastrointestinal disorders	1046	47.8	594	27.2
Hepatobiliary disorders	72	3.29	46	2.10
Skin and subcutaneous tissue disorders	984	45.0	461	21.1
Musculoskeletal and connective tissue disorders	426	19.5	119	5.44
Renal and urinary disorders	71	3.23	32	1.46
Reproductive system and breast disorders	77	3.52	41	1.87
Congenital familial and genetic disorders	7	0.33	0	0
General disorders and administration site conditions	297	13.6	203	9.28
Investigations	2207	100.9	1723	78.8
Injury, poisoning, and procedural complications	448	20.5	19	0.87
Surgical and medical procedures	2	0.09	0	0

SOC Medical Dictionary for Regulatory Activities (MedDRA) system organ class (MedDRA ver. 8.0)

Table 3 Major infections and infestations (≥1.0 events/100 pt-yr)

PT	Adverse events	
	Number of events	Events/ 100 patient-years
Total	2696	123.2
Nasopharyngitis	1402	64.1
Pharyngitis	89	4.07
Cystitis	85	3.88
Gastroenteritis	69	3.15
Tinea infection	67	3.06
Herpes simplex	61	2.79
Bronchitis acute	60	2.74
Pneumonia	56	2.56
Dental caries	53	2.42
Upper respiratory tract infection	53	2.42
Herpes zoster	50	2.29
Paronychia	41	1.87
Bronchitis	34	1.55
Tinea pedis	33	1.51
Urinary tract infection	32	1.46
Sinusitis	30	1.37
Cellulitis	29	1.33
Influenza	25	1.14
Purulence	22	1.01

PT MedDRA preferred term according to MedDRA (ver. 8.0)

pneumonia, 48% of the AEs were reported as serious events. Long-term exposure did not increase the incidence of serious infections (Fig. 3a). The onset of pneumonia tended to increase in the winter, while the onset of urinary tract infection increased in the summer (Fig. 3b, c). When the incidences of infections were analyzed using pooled data from three randomized controlled studies (one phase II study and two phase III studies [8–10]), the incidence in the TCZ-treated patients (41.9%) was not significantly higher than that in the control group (37.6%). Two cases of TB were reported (one pulmonary, one miliary TB); these developed 1.5 and 2.5 years after TCZ treatment initiation, respectively. One patient had a positive PPD skin test (no prophylaxis reported), and the other had, in retrospect, a suspicious chest X-ray during the pre-treatment period. Thus, reactivation of existing TB may have occurred. Both patients improved with the appropriate treatment, but they withdrew from the studies after developing TB.

Gastrointestinal perforation occurred in five patients, and a causal relationship with TCZ could not be ruled out in three cases. All patients improved after receiving the appropriate treatment. Nineteen malignancies were reported in 19 patients (3.2%, 0.8/100 pt-yr), with breast cancer and colon carcinoma observed in more than two patients, respectively (Table 5). No patients developed systemic lupus erythematosus or any other additional autoimmune disease.

Most of the abnormal laboratory test results were minor. Decreases in the leukocyte count to the low normal range were observed a few days after TCZ administration. Although grade 2 (<1500–1000/μL) and grade 3 neutropenia (<1000–500/μL) were observed in 92 (15.3%) and 36 patients (6.0%), respectively, these events were all transient, and no patients experienced febrile neutropenia or withdrew from a study due to neutropenia. Transient liver function disorders were also reported. Alanine aminotransferase (ALT) increased to grade 3 [>5.0–20.0 × ULN (upper limit of normal)] in 16 patients (2.7%), to grade 2 (>2.5–5.0 × ULN) in 31 patients (5.2%), and to grade 1 (>ULN–2.5 × ULN) in 221 patients (36.8%). Aspartate aminotransferase (AST) increased to grade 3 (>5.0–20.0 × ULN) in seven patients (1.2%), to grade 2 (>2.5–5.0 × ULN) in 17 patients (2.8%), and to grade 1 (>ULN–2.5 × ULN) in 180 patients (30.0%). There were no grade 4 (>20.0 × ULN) ALT or AST values and no serious liver function disorders, such as fulminant hepatitis, during the TCZ treatment. Total bilirubin increased to grade 3 (>3.0–10.0 × ULN) in three patients (2.7%), to grade 2 (>1.5–3.0 × ULN) in 32 patients (5.3%), and to grade 1 (>ULN–1.5 × ULN) in 186 patients (30.9%). There were no severe AEs related to these abnormal values. Mean non-fasting total blood cholesterol (TC) increased soon after treatment initiation and then stabilized (185 mg/dL at baseline; 215 mg/dL at 1 year; 210 mg/dL at 5 years) (Fig. 4a, b). As high-density lipoprotein cholesterol (HDLC) followed a similar pattern, the atherogenic index [(TC – HDLC)/HDLC] did not change (Fig. 4c, d). In total, 173 patients (28.8%) received statin treatment after starting TCZ therapy. Mean values of total and low-density lipoprotein cholesterol (LDLC) levels at baseline were higher in the statin-treated group than in the untreated group, suggesting that the former may have had risk factors before initiating the TCZ treatment. Lipid abnormalities were controllable by statin treatment (Fig. 5).

Efficacy

The ACR response rates rapidly increased during the first year of TCZ treatment. The ACR20 (20% improvement according to the ACR criteria) then became stable, while the ACR50 and ACR70 (50 and 70% improvement) continued to increase (Fig. 6a). At 5 years, 91.3, 73.0, and 51.3% of patients had achieved ACR20, ACR50, and ACR70, respectively, and 59.7% of the patients had achieved DAS28 remission (Fig. 6b). At 6 months, >90% of patients had achieved a DAS28 EULAR moderate or good response (Fig. 6c), and this level was maintained during the study period. The mHAQ score also improved during the study period (Fig. 6d). Although ACR response